Cumhuriyet Sci. J., 44(1) (2023) 90-98
DOI: https://doi.org/10.17776/csj.1223357

Cumhuriyet Science Journal

| csj.cumhuriyet.edu.tr | Founded: 2002 ISSN: 2587-2680 e-ISSN: 2587-246X Publisher: Sivas Cumhuriyet University

Biosynthesis, Characterization and Antioxidant Properties of ZnO Nanoparticles Using Punica Granatum Peel Extract as Reducing Agent

Zehra Seba Keskin [1,a,*], Ünsal Açıkel [2,b]

[1] *Health Services Vocational School, Department of Pharmacy, Sivas Cumhuriyet University, Sivas, Türkiye.*
[2] *Department of Chemical Engineering, Sivas Cumhuriyet University, Sivas, Türkiye.*
**Corresponding author*

Research Article

History
Received: 23/12/2022
Accepted: 02/03/2023

ABSTRACT

The green synthesis method of nanoparticles using plant extracts attracts great attention as a reliable, low-cost, sustainable, environmentally friendly protocol that prevents or minimizes waste generation. In this study, *Punica granatum* peel extract was used as the reducing plant material and zinc acetate dihydrate ($Zn(CH_3COO)_2.2H_2O$) solution was used as the starting metal. In the synthesis, optimum conditions were determined by UV visible spectroscopy using different metal ion concentrations, plant extract amount, temperature, and pH parameters. For characterization of ZnONPs synthesized at optimum conditions, Scanning Electron Microscopy (SEM), Energy Dispersive X-ray spectroscopy (EDX), X-ray diffraction (XRD), Fourier Transform Infrared spectroscopy (FTIR), Dynamic Light Scattering (DLS), Zeta potential and Atomic Force Microscope (AFM) analyzes were made. It has been determined that the synthesized ZnONPs are spherical, have good stability, high purity, and nanoscale. The free radical scavenging capacity of biosynthesized ZnONPs was evaluated by DPPH analysis with different concentrations. The IC50 value was determined as 250µg ml^{-1}.

Keywords: Neuropathic pain, L-759,633, SER 601, Hot plate, Pregabalin.

[a] zkeskin@cumhuriyet.edu.tr https://orcid.org/0000-0003-1334-5158 [b] uacikel@cumhuriyet.edu.tr https://orcid.org/0000-0003-4969-8502

Introduction

Nanotechnology is a new and rapidly developing technology field that enables applications such as processing, measurement, design, modeling, and arrangement performed on materials between 1-100 nm, aiming to provide advanced features at the atomic and molecular level or completely new physical, chemical and biological properties to the substance [1]. Considered as the building block of nanotechnology, nanoparticles (NP) describe a broad class of materials that contain particulate matter with a size less than 100 nm [2].

In recent years, biological methods are preferred as an alternative to chemical and physical methods in synthesizing metal oxide nanoparticles. Biological methods increase the efficiency of the process by catalyzing reactions in aqueous media at standard temperature and pressure. Also, they have the advantage of increasing the flexibility of the process by being applied in almost any environment and at any scale [3]. The green synthesis method involves the reduction of metal ions using biomass/extract, such as bacteria, fungi, yeast, virus, microalgae, and plant as an extracellular or intracellular source of reducing agents (see [4] and the references therein) The use of plant biomass/extracts instead of other biomaterials has advantages such as eliminating the detailed maintenance of cell cultures, rapid synthesis, finding various metabolites that can aid reduction, being easily accessible [5], [6]. In various studies in the literature, it has been stated that compounds found in plants such as polyphenols, proteins, terpenoids, alkaloids, amino acids, alcoholic compounds, glutathions, polysaccharides, antioxidants, organic acids, contribute to the reduction of metal ions to nanoparticles and to ensure their stability [7, 8].

Within the large metal oxide nanoparticle family, ZnONPs have an important potential in various applications such as electronics, communication, sensor, cosmetics, environmental protection, biology, and medical industry [9] due to the properties antifungal, antibacterial, antiviral, wound healing, high catalytic and photochemical activity, UV filtering, optical. Besides, the US FDA recognizes ZnO as a GRAS (generally considered safe) metal oxide (see [10]. and the references therein).

Punica granatum L. is a perennial plant belonging to the genus Punica of the Lythraceae family [11]. The peel, which constitutes 50% of the fruit weight, is a good source of high molecular weight phenolics, elagitanen, proanthocyanidins, complex polysaccharides, flavonoids, and microelements and has strong antimutagenic, antioxidant, and antimicrobial properties [12]. Various studies have reported that polyphenolic and flavonoid compounds act as reducing, stabilizing, limiting growth, and preventing agglomeration during the production of nanoparticles by biosynthesis (see [13] and the references therein).

The aim of this study is to synthesize ZnONPs using *Punica granatum* peel extract as a reducing and stabilizing agent and to determine the antioxidant activities of biosynthesized nanoparticles. Optimum conditions of the reaction in different parameters such as plant extract amount, metal ion concentration, temperature, and pH

were determined by UV-visible spectrophotometer. All properties of ZnONPs synthesized at optimum conditions were investigated in detail with Scanning Electron Microscopy (SEM), Energy Dispersive X-ray analysis (EDX), Zeta Potential, Dynamic Light Scattering (DLS), Fourier Transform Infrared Spectroscopy (FTIR), X-Ray Diffraction (XRD) and Atomic Force Microscopy (AFM) analyzes to be used in bionanocomposites in later studies.

Materials and Methods

Preparation of Pomegranate (Punica granatum) Peel Extract

The fruits obtained from local markets in Sivas/Turkey were washed several times to remove dust, then peel and inner parts were separated and dried in the laboratory for 2 weeks. *Punica granatum* fruit peels extract was obtained by boiling 5 g of powdered peel in 100 ml of sterile distilled water in 250 ml of flask until it turns yellow-brown for 15 minutes. Then it was cooled to room temperature and filtered with filter paper Whatman No. 1 and stored at +4 ^{o}C in a refrigerator to be used for further experiments.

Synthesis of ZnONPs by green method

50 ml of 0.15 M $Zn(CH_3COO)_2.2H_2O$ solution was prepared. 10 ml of fruit peel extract was added drop by drop to this prepared solution and adjusted to pH 12 with 1 M NaOH and mixed in a magnetic stirrer for 2 hours. The extract, which was initially yellow-brown in color, turned into a light yellow mixture [14]. This mixture was centrifuged at 10.000 rpm for 10 minutes and then dried at 50 ^{o}C for 2 days [15].

Determination of Optimum Synthesis Conditions of ZnONPs

In some studies, it has been reported that the optimum synthesis conditions in the green synthesis method are determined by changing the parameters such as plant extract amount, metal ion solution concentration, incubation time, medium pH and temperature [16, 17]. During the synthesis, different metal ion solution concentrations of 0,03 M, 0,05 M, 0,1 M, 0,15 M, and 0,2 M were applied by keeping the plant extract amount, incubation time, medium pH and temperature constant. To determine the optimum amount of plant extract, 2 ml, 4 ml, 6 ml, 8 ml, and 10 ml of extract were added to 50 ml of zinc acetate dihydrate solution. Keeping the other parameters the same, the pH value of the environment was brought to 9, 10, 11, and 12 and the optimum pH value was determined. Finally, synthesis was carried out at 20 ^{o}C, 40 ^{o}C, 50 ^{o}C and 60 ^{o}C to determine the optimum reaction temperature for NP synthesis.

UV–Visible Absorption Spectroscopy

UV-visible spectroscopy is a widely used technique for determining the optical properties of metallic nanoparticles [18]. Since the extract and nanoparticle solution was dark and concentrated, dilution was made before UV analysis was performed. After diluting these solutions with distilled water at a ratio of 1/40, they were placed in a quartz cuvette and their optical properties were determined in the UV-Vis spectrophotometer (UV-2600, Shımadzu) in the wavelength range of 200 to 900 nm.

X-ray Diffraction (XRD)

XRD is a characterization method used for phase identification and characterization of the crystal structure of nanoparticles [19]. XRD measurements of synthesized ZnONPs were made in X-Ray Diffractometer (Rigaku Miniflex 600). XRD shapes were obtained with a step size of 0.05 between Cu-Kα radiation (k = 1.54 A) and 2θ = 10 °-90 ° values. Crystal sizes of the nanoparticles were calculated using the Debye-Scherrer formula.

Scanning Electron Microscopy (SEM) and Energy-Dispersive X-ray Analysis (EDS)

SEM analysis to determine the structure, shape, and size of ZnONPs obtained by the green synthesis method and EDX analysis to determine the basic composition of the NPs were obtained by using Scanning Electron Microscope (TESCAN MIRA 3 XMU). Before analysis, the samples were plated with gold in an automatic coater. This process increases the surface conductivity and provides better quality images.

Fourier-Transform Infrared Spectroscopy (FTIR)

FT-IR spectrum was used to define functional groups in ZnONPs obtained by green synthesis method and *Punica granatum* peel extract used as a reducing agent. The FT-IR spectrum of the extract and ZnONPs was realized with Bruker Tensor II and adjusted to work at 2 cm^{-1} resolution in the range of 400-4000 cm^{-1} to obtain a good signal/noise ratio.

Dynamic Light Scattering (DLS) Analysis

Average size, size distribution, and polydispersity index (PDI) measurements of the synthesized nanoparticles were made with Malvern Brand, Zetasizer model particle size analysis device. After diluting the nanoparticles with pure water, the sonication process was applied for 15 minutes to disintegrate the agglomerated structures, and analysis was performed by placing them in 1.5 ml cuvettes.

Zeta Potential Analysis

Zeta potential analysis was performed with the Malvern, Nano ZS Model zeta sizer device to determine the colloidal distribution stability of ZnONPs. Measurements were made at 25 °C with a back reflection angle of 173°. The nanoparticles prepared for analysis were diluted with distilled water, taken with a syringe in 1 ml, and placed in disposable zeta potential cells, and measurements were made.

Atomic Force Microscopy

The particle size, distribution, and morphology of nanoparticles were analyzed using atomic force microscope (Veeco Multimode 8). The prepared nanoparticle solutions were diluted at a ratio of 1/100, then spread a drop on a clean glass surface with a size of 1 cm x 1 cm and dried. The surface topographies of the nanoparticle sample prepared in this way were scanned in 2D and 3D in an area of 3x3 μm^2 and 20x20 μm^2.

Antioxidant Assay (DPPH Free Radical Scavenging)

The radical scavenging activities of *Punica granatum* extract and biosynthesized ZnONPs were determined by the method reported by Sathiskumar et al. [20]. Samples were prepared at different concentrations (50,75, 100, 250 and 500 µg/mL) for ZnONPs, extract and Ascorbic acid (as positive control). Then, 1 ml of each sample at different concentrations was added to 2 ml of 0.1 mM DPPH (in ethanol) solution. After 30 minutes of incubation in the dark, absorbance values were measured at 517 nm in a UV spectrophotometer. The radical scavenging activity was determined using equation 1 given below.

$$Sc\ (\%) = (1-(As/Ac))*100 \quad [1]$$

Here, Sc represents the DPPH scavenging activity (%), Ac represents the absorbance of the positive control, and As represents the absorbance of the sample.

Results and Discussion

Visual Observation and UV–visible spectroscopy

The visual color change is accepted as a preliminary test to confirm the formation of NPs obtained by green synthesis. The first indication of the reduction of Zn ions to ZnONPs by the *Punica granatum* peel extract was determined as the yellow-brown color of the extract turning into a light yellow color.

Determination of Optimum Zinc Acetate Dihydrate [$Zn(CH3COO)_2$].$2H_2O$ Concentration

In this study, the effect of different zinc acetate dihydrate concentrations (0,03 M, 0,05 M, 0,1 M, 0,15 M, and 0,2 M) on the formation of ZnONPs obtained by green synthesis was determined by UV-visible absorption spectroscopy. While no absorption peak was observed at 0,03 M, 0,05 M, and 0,1 M (Figure 1a), the maximum absorbance peak was determined at a concentration of 0,15 M. This peak read at 358 nm confirms the synthesis since it is the characteristic peak of ZnONPs. However, despite the increase in 0,2 M zinc acetate dihydrate concentration, it was observed that there was a decrease in absorbance and an expansion at the peak point. Therefore, it is concluded that increasing the metal ion concentration to the optimum level will increase the NP formation while increasing the metal ion concentration will decrease the NP formation.

Determining the Optimum Extract Amount

In the synthesis of ZnONPs, *P. granatum* extract was used as a stabilizing, reducing, and capping agent. In the optimization study for biosynthesis, the effect of the amount of extract on absorption and peak priority was observed by UV-Vis absorption spectroscopy. 2 ml, 4 ml, 6 ml, 8 ml, and 10 ml of extract were added to 0,15 M Zn $(CH_3COO)_2.2H_2O$ used as the starting solution and UV spectra of the solutions were obtained as a result of the reaction. As seen in Figure 1b, it was determined that the maximum absorbance peak occurred at 356 nm and 10 ml extract usage. In some studies, it has been stated that by increasing the plant extract rate, the NP synthesis rate increases in direct proportion [21, 22].

Determining the Optimum Temperature

It is known that the temperature of the reaction medium is an important factor regulating the structure of the synthesized nanoparticles [21]. To determine the optimum reaction temperature of the synthesis using 0,15 M Zn $(CH_3COO)_2.2H_2O$ solution and 10 ml extract, the synthesis was carried out at 20 ^{O}C, 40 ^{O}C, 50 ^{O}C, and 60 ^{O}C. In the UV spectrum seen in Figure 1c, it is seen that the absorbance peak intensities increase as the temperature increases.

The highest absorbance peak determined at 60 ^{O}C and 344 nm shows that zinc acetate is converted into ZnONPs. Synthesis of ZnONPs performed at higher rates at higher temperatures has been reported in various studies in the literature [23, 24].

Determining the Optimum pH Value

The pH of the medium is an important parameter affecting the NP size. During the synthesis, it has been noted that there is an increase in the absorbance value as a result of the pH increase from 9 to 12. This event is due to the formation of nucleation centers that increase with the increase of pH. As the nucleation center increases, the reduction of metallic ions to metal nanoparticles also increases [25]. While no absorption peak was observed at pH 9 and pH 10, the characteristic maximum absorption peak was observed at 358 nm at pH 12 (Figure 1d) . These results are consistent with studies in the literature [17, 23].

While the characteristic absorption peak of ZnONPs solution synthesized at specified optimum conditions was determined at 359 nm, no peak of peel extract was observed (Figure 2).

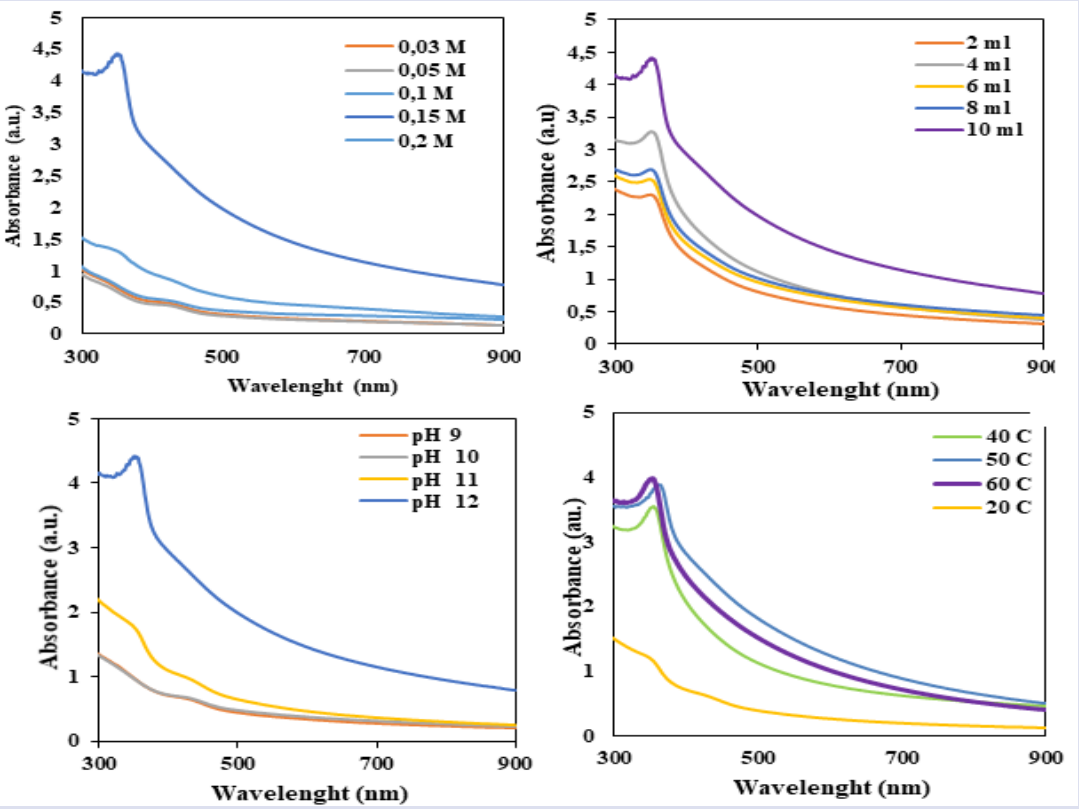

Figure1. Optimization of synthesis parameters, a. zinc acetate concentrations, b. amount of extract, c. pH. d. Temperature

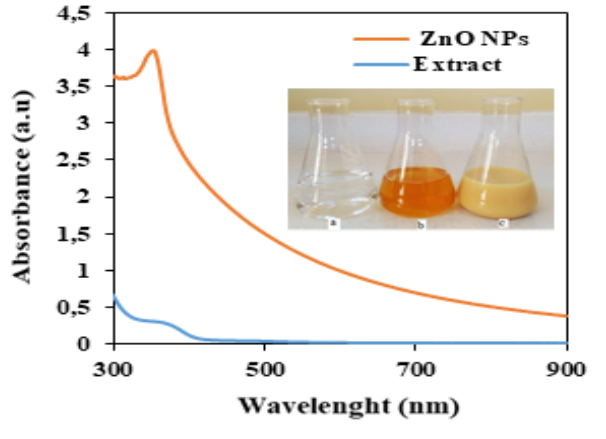

Figure 2. Synthesis of ZnONPs in optimum conditions

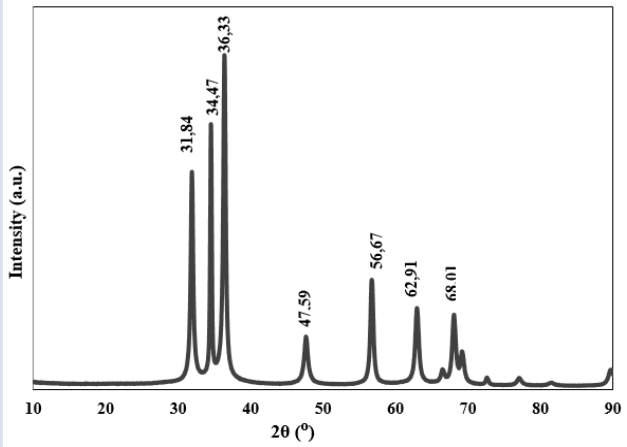

Figure 3. XRD graph of synthesized ZnONPs

XRD

The XRD diffraction peaks of the ZnONPs samples obtained by the green synthesis method are shown in Figure 3. It was determined that the characteristic peaks observed at 2θ=31,84°, 34,47°, 36,33°, 47,59°, 56,67°, 62,91, 68,01 of the ZnONPs correspond to the planes (100), (002), (101), (102), (110), (103) and (112), respectively. These obtained data match the card numbered JCPDS Data Card No: 36–1451 in the Joint Committee on Powder Diffraction Standards (JCPDS) database [26]. Besides, since all the peaks seen in the graphic are characteristic peaks of ZnO, it confirms that they do not contain impurities.

Crystal size measurement for synthesized ZnONPs was calculated using the Debye-Scherrer equation [2] [27].

$$D = \frac{K\lambda}{\beta \cos\theta} \qquad [2]$$

D: crystal size,
K: Debye Scherrer constant (0.94)
λ: Cu-Kα radiation (1.54 A),
β: half-length width of maximum peak (FWHM),
θ: It is the Bragg angle value obtained from the 2θ value of the maximum peak in the XRD diffraction pattern.

The average crystal size of ZnONPs was calculated as approximately 19.51 nm according to the Debye-Scherrer formula [2]. FWHM values for each peak point determined to calculate particle size are shown in Table 1.

Table 1. Crystal sizes and peak values of ZnONPs

2 θ	h k l	FWHM	D(nm)
31,84	100	0,49192	17,55
34,47	002	0,29878	29,10
36,33	101	0,5026	17,39
47,59	102	0,67818	13,38
56,67	110	0,53313	17,70
62,91	103	0,63896	15,23
68,01	112	0,63676	15,73

SEM and EDX

The structure, shape, and size of ZnONPs obtained by the green synthesis method were determined by SEM images (Figure 4). SEM images obtained with 50 kx and 200 kx magnifications show that synthesized ZnONPs have a spherical structure and particle sizes in the range of 33.6 nm and 51.47 nm. The obtained results are similar to some studies in the literatüre [28, 29].

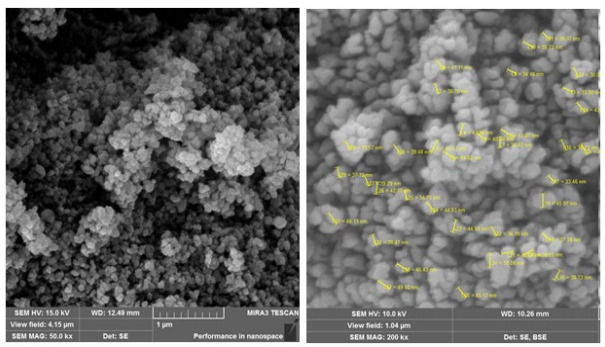

Figure 4. SEM image of ZnONPs

Chemical purity, elemental composition, and stoichiometry of ZnONPs were determined by EDX analysis. In EDX spectra shown in Figure 5, it is seen that the peaks belong only to Zn and O. Therefore, it is confirmed that the synthesized ZnONPs are of high purity. The stoichiometric mass percentage for Zn and O were determined 76.77% and 23.23%, respectively. These results are seen to be consistent with the results of other studies in the literature [15, 30, 31].

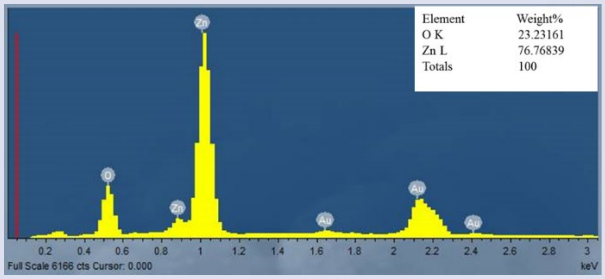

Figure 5. EDX spectrum of ZnONPs

FTIR

FTIR spectrum analysis shows the relationship of absorption bands with chemical compounds in pomegranate peel and ZnONPs. The availability of functional groups in ZnONPs is given in Figure 6. In the spectrum, absorption peaks are seen at 3219 cm^{-1}, 1578 cm^{-1}, 1399 cm^{-1},1088 cm^{-1}, 1032 cm^{-1}, 841 cm^{-1}, 717 cm^{-1} and 480 cm^{-1}. The wide peak observed at 3219 cm^{-1} is due to O-H stress vibrations. While the peak at 1578 cm^{-1} corresponds to C = C stress in aromatic rings and C = O stress in polyphenols, it is thought that the absorption peak at 1399 cm^{-1} is caused by the C = N amide-1 stress in the protein. The peak at 1088 cm^{-1} showed the C-O stretch in amino acid and the peak at 1032 cm^{-1} showed the presence of the C-N stretch [15]. Also, in the spectrum, it was determined that peaks were formed at 841 cm^{-1} and 717 cm^{-1} correspondings to the C-H stretching of alkanes [17]. Metal oxides form an absorption peak in the region between 600 - 400 cm^{-1} due to interatomic vibrations.

The characteristic peak corresponding to the ZnO stretch band showing ZnO formation, which is stated in the literature, was observed at a wavenumber of 481 cm^{-1} [32]. Therefore, it is confirmed that the water-soluble compounds in *Punica granatum* peel extract are effective in determining the shape of nanoparticles and in reducing metal ions.

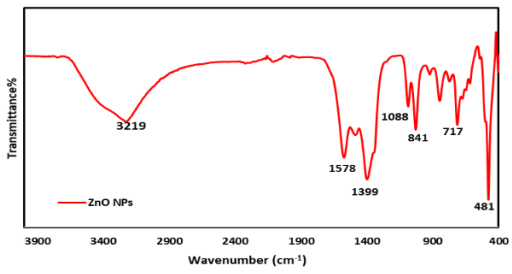

Figure 6. FTIR spectrum for ZnONPs

DLS Analysis Results

The size distribution, average particle size, and *polydispersity index* (PDI) of ZnONPs synthesized by the green method were determined by the dynamic light scattering method. The size distribution of ZnONPs is shown in Figure7. The average particle size for ZnONPs in solution was found to be 348 nm with DLS. It was determined that the ZnONPs size obtained by DLS was higher than the average NP size determined in SEM images. This is thought to be because the NP size measured by DLS is the hydrodynamic diameter of the particle swollen with water or solvent, while the value measured by SEM corresponds to the dried NP size. Another reason can be shown as the measurement of clustered particle sizes rather than individual particle sizes since NPs tend to coalesce in an aqueous medium [33].The PDI value, which is a dimensionless value, ranges from 0.01 to 0.5-0.7 for monodisperse particles, while the PDI value for particles with very wide size distribution is

greater than 0.7 [34]. The fact that the PDI value of ZnONPs synthesized in the study was 0.457 shows that ZnONPs are monodisperse. In addition, it was determined that the ZnO NP size obtained with DLS was higher than the average NP size determined in SEM images. This is because the NP size measured by DLS is not water or solvent dependent. It is the hydrodynamic diameter of the particle swollen by SEM, while the value measured by SEM is considered to correspond to the dried NP size. Another reason can be cited as a measurement of aggregated particle sizes rather than individual particle sizes, as NPs tend to coalesce in aqueous media [33].

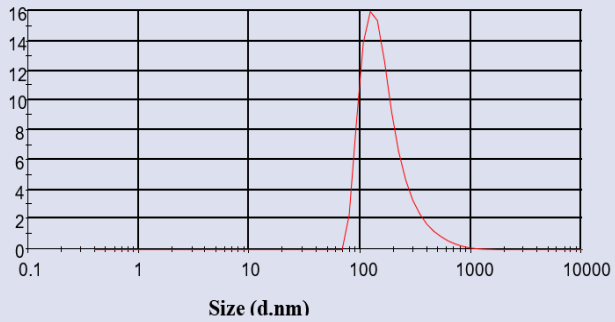

Figure 7. Size distribution of ZnONPs

Stability of ZnONPs

Zeta potential analysis was performed to determine the potential stability depending on the NP surface charges and the electrostatic repulsive forces between the NPs. The zeta potential of colloidal ZnONPs synthesized by the green method was found to be -46.0 mV as seen in Figure 8.

The negatively charged surface of the nanoparticles confirms the repulsion between particles and proves that it results in stable suspensions [35]. Because agglomeration/aggregation seen between NPs occurs due to van der Waals forces and chemical bonding [36].

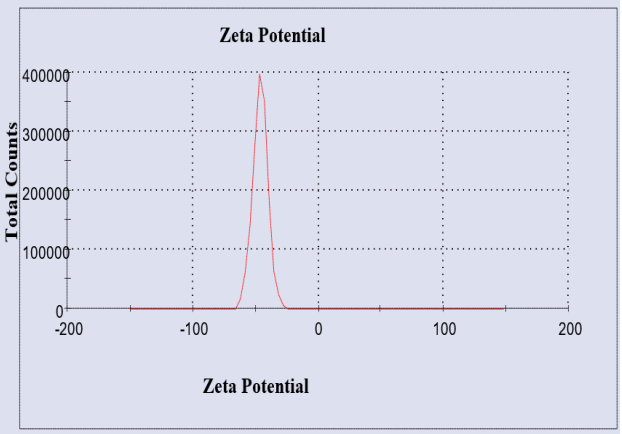

Figure 8. Zeta potential of synthesized ZnONPs

AFM

One of the characterizations that enable us to determine the morphology and size of the synthesized ZnONPs is the atomic force microscope with high resolution.

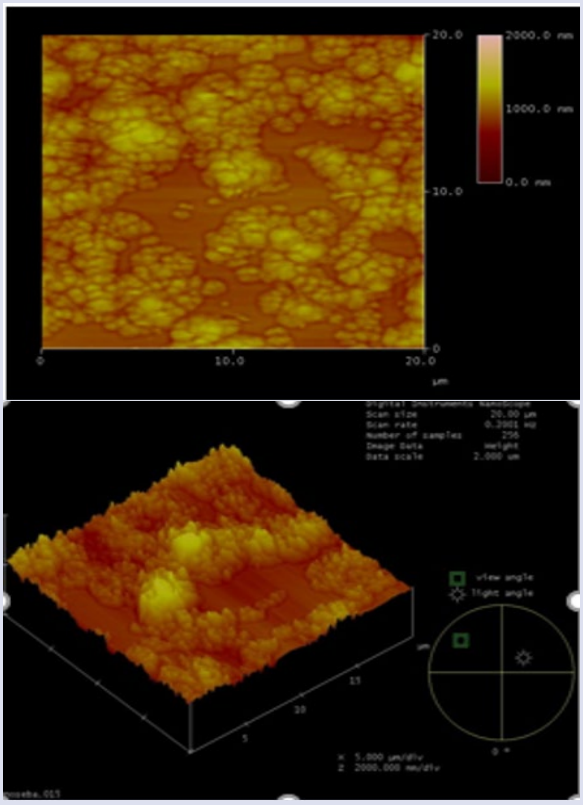

Figure 9. AFM images of ZnONPs at 20x20 µm^2 a) 2D b) 3D

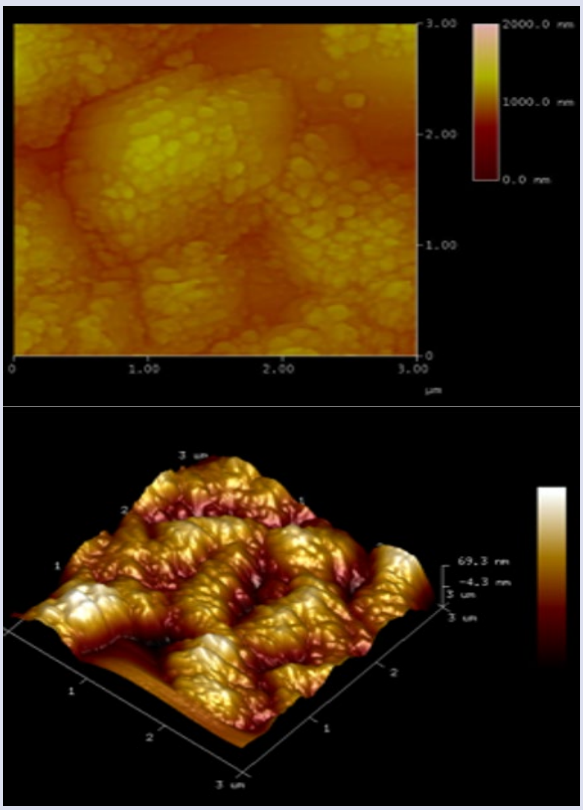

Figure 10. AFM images of ZnONPs at 3x3 µm^2 a) 2D b) 3D

2D and 3D surface images and surface roughness values were obtained by scanning NPs with magnification ranges of 20x20 μm^2 and 3x3 μm^2 (Figure 9- 10). When 2D and 3D images with a magnification range of 3x3 μm^2, which give the NP size, were examined, the size of the largest nanoparticle in the 3D image was determined to be 69,3 nm. The average roughness value (Ra) of the nanoparticles was measured as 19,88 nm, and the maximum roughness value (Rmax) was 201,55 nm.

Antioxidant Activity

In this study, antioxidant capacity of *Punica granatum* peel extract and biosynthesized ZnONPs was investigated by DPPH method. As seen in Figure 11, ZnONPs and Ascorbic acid used as a control produced strong inhibitory activity against DPPH radical. It was determined that the free radical scavenging activities increased as the ZnONPs concentration increased. The % inhibition values of 250 µg/ml and 500 µg/ml concentrations of ZnONPs (92.3% and 93.3%, respectively) showed strong antioxidant capacity when compared with ascorbic acid. It is known that the significant antioxidant potential of ZnONPs is due to the hydrogen donating abilities of active phytochemicals such as alkaloids, anthocyanins, anthocyanidins, tannins, flavonoids, phenolics, proanthocyanidins, sterols, terpenes, and xanthonoids in *Punica granatum* peel [19]. As seen in Table 2, the IC_{50} value of biosynthesized ZnONPs falls within the range of IC_{50} values of previously studied ZnONPs.

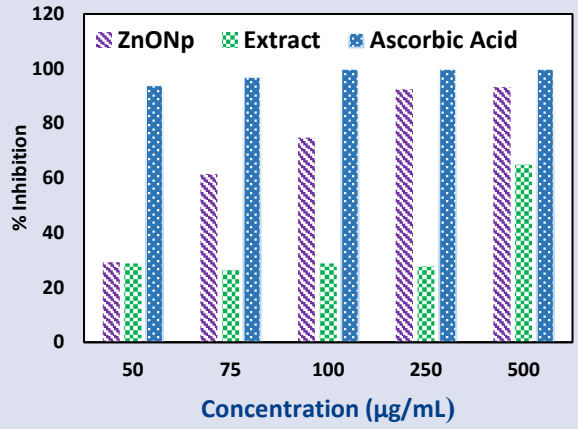

Figure 11. DPPH radical scavenging activity of ZnONPs, extract of *Punica granatum* and ascorbic acid

Table 2. The comparison of DPPH radical scavenging activity of synthesized ZnONPs of the present study with other biosynthesized ZnONPs

ZnONPs	IC_{50} (µg/ml)	Reference
ZnONPs –*Beta vulgaris*	4400	[37]
ZnONPs-*Mussaenda frondosa*	857	[38]
ZnONPs- *Citrullus colocynthis*	290	[39]
ZnONPs- *Punica granatum*	250	This present
ZnONPs-*Lutfa acutangula*	134,12	[40]
ZnONPs-*Coccinia abyssinica*	127,74	[41]

Conclusions

In this study, ZnONPs was synthesized by green synthesis method using *Punica granatum* peel extract, which is food waste. The characterizations of ZnONPs synthesized at optimum conditions were made by SEM, EDX, XRD, FTIR, DLS, zeta potential, and AFM analysis. The sizes of the NPs, which are seen to be in spherical structure in SEM images, were determined to be between 33.6 nm and 51.47 nm, and it was confirmed that they do not contain impurities with the results of XRD and EDX analysis. Besides, the high negative zeta potential value (-46 mV) determined for the ZnONPs proves that the NPs have good stability, as it shows the repulsive force between the particles. The IC_{50} value of biosynthesized ZnONPs was found to be 250 µg ml^{-1} by DPPH analysis. It was determined that it has strong antioxidant activity from % inhibition values.

As a result, a clean, antioxidant, environmentally friendly, inexpensive, the non-toxic approach is reported for the synthesis of zinc oxide nanoparticles.

Acknowledgment

The **PhD** thesis research process was supported by the Scientific Research Project Fund Sivas Cumhuriyet University (Grant No. M-721).

Conflicts of interest

The authors declare that they have no conflict of interest.

References

[1] Beykaya M., Çağlar A. Bitkisel özütler kullanılarak gümüş-nanopartikül (AgNP) sentezlenmesi ve antimikrobiyal etkinlikleri üzerine bir araştırma, *Afyon Kocatepe Üniversitesi Fen ve Mühendislik Bilimleri Dergisi*, *16* (3) (2016) 631-641.

[2] Laurent S., Forge D., Port M., Roch A., Robic C., Vander Elst L., Muller R. N., Magnetic iron oxide nanoparticles: synthesis, stabilization, vectorization, physicochemical characterizations, and biological applications, *Chemical Reviews*, *108* (6) (2008) 2064-2110.

[3] Schröfel A., Kratošová G., Šafařík I., Šafaříková M., Raška I., Shor L. M., Applications of biosynthesized metallic nanoparticles–a review, *Acta Biomaterialia*, *10*(10) (2014) 4023-4042.

[4] Shah M., Fawcett D., Sharma S., Tripathy S. K., Poinern G. E. J., Green synthesis of metallic nanoparticles via biological entities, *Materials*, *8* (11) (2015) 7278-7308.

[5] Iravani S., Green synthesis of metal nanoparticles using plants, *Green Chemistry*, *13* (10) (2011) 2638-2650.

[6] Shankar S. S., Rai A., Ahmad A., Sastry M., Rapid synthesis of Au, Ag, and bimetallic Au core–Ag shell nanoparticles using Neem (Azadirachta indica) leaf broth, *Journal of Colloid and Interface Science*, *275* (2) (2004) 496-502.

[7] Asmathunisha N., Kathiresan K., A review on biosynthesis of nanoparticles by marine organisms, *Colloids and Surfaces B: Biointerfaces*, *103* (2013) 283-287.

[8] Canbaz G. T., Açıkel U., Açıkel Y. S., ZnO-Kitosan Kompoziti ile Ağır Metal Giderimi, *Avrupa Bilim ve Teknoloji Dergisi*, (35) (2022) 603-609.

[9] Sharma D., Sabela M. I., Kanchi S., Mdluli P. S., Singh G., Stenström T. A., Bisetty K., Biosynthesis of ZnO nanoparticles using Jacaranda mimosifolia flowers extract: synergistic antibacterial activity and molecular simulated facet specific adsorption studies., *Journal of Photochemistry and Photobiology B: Biology*, *162* (2016) 199-207.

[10] Ghaseminezhad S. M., Hamedi S., Shojaosadati S. A. Green synthesis of silver nanoparticles by a novel method: Comparative study of their properties, *Carbohydrate Polymers*, *89* (2) (2012) 467-472.

[11] Çetinkaya H. K., Güvercin D., Karakurt Y., Molecular characterization of pomegranate (*Punica granatum* L.) Genotypes with SSR Markers, *Süleyman Demirel Üniversitesi Fen Edebiyat Fakültesi Fen Dergisi*, *14* (2) (2019) 345-351.

[12] Okumuş G., Yıldız E., Bayizid A. A., Doğal antioksidan bileşikler: Nar yan ürünlerinin antioksidan olarak değerlendirilmesi, *Uludağ Üniversitesi Ziraat Fakültesi Dergisi*, *29* (2) (2015).

[13] Vijayaraghavan K., Ashokkumar T., Plant-mediated biosynthesis of metallic nanoparticles: a review of literature, factors affecting synthesis, characterization techniques and applications, *Journal of Environmental Chemical Engineering*, *5* (5) (2017) 4866-4883.

[14] Dobrucka R., Długaszewska J., Biosynthesis and antibacterial activity of ZnO nanoparticles using Trifolium pratense flower extract, *Saudi J Biol Sci* 23 (2016) 517–523.

[15] Yedurkar S. M., Maurya C. B., Mahanwar P. A., A biological approach for the synthesis of copper oxide nanoparticles by Ixora coccinea leaf extract, *J. Mater. Environ. Sci*, *8* (4) (2017) 1173-1178.

[16] Bhuyan T., Mishra K., Khanuja M., Prasad R., Varma A., Biosynthesis of zinc oxide nanoparticles from Azadirachta indica for antibacterial and photocatalytic applications, *Materials Science in Semiconductor Processing*, *32* (2015) 55-61.

[17] Gupta M., Tomar R. S., Kaushik S., Mishra R. K., Sharma D., Effective antimicrobial activity of green ZnO nano particles of Catharanthus roseus, *Frontiers in Microbiology*, *9*, (2018) 2030.

[18] Pal S., Tak Y. K. Y Song J. M., Does the antibacterial activity of silver nanoparticles depend on the shape of the nanoparticle? A study of the gram-negative bacterium Escherichia coli., *Appl Environ Microbiol*, *73* (6) (2007) 1712-1720.

[19] Sun S., Murray C. B., Weller D., Folks L., Moser A., Monodisperse Fe Pt nanoparticles and ferromagnetic Fe Pt nanocrystal superlattices, *Science*, *287*(5460) (2000) 1989-1992.

[20] Sathishkumar G., Pradeep K. Jha, Vignesh V., Rajkuberan C., Jeyaraj M., Selvakumar M., Rakhi Jha, Sivaramakrishnan S., Cannonball fruit (Couroupita guianensis, Aubl.) extract mediated synthesis of gold nanoparticles and evaluation of its antioxidant activity, *Journal of Molecular Liquids* 21 (2016) 229–236.

[21] Mittal J., Batra A., Singh A., Sharma M. M., Phytofabrication of nanoparticles through plant as nanofactories, *Advances in Natural Sciences: Nanoscience and Nanotechnology*, *5* (4) (2014) 043002.

[22] Song J. Y., Kwon E. Y., Kim B. S., Biological synthesis of platinum nanoparticles using Diopyros kaki leaf extract. *Bioprocess and Biosystems Engineering*, *33* (1) (2010) 159-164.

[23] Jamdagni P., Khatri P., Rana J. S., Green synthesis of zinc oxide nanoparticles using flower extract of Nyctanthes arbor-tristis and their antifungal activity, *Journal of King Saud University-Science*, *30* (2) (2018) 168-175.

[24] Chunfa D., Fei C., Xianglin Z., Xiangjie W., Xiuzhi Y., Bin Y., Rapid and green synthesis of monodisperse silver nanoparticles using mulberry leaf extract, *Rare Metal Materials and Engineering*, *47* (4) (2018) 1089-1095.

[25] Bali R., Harris A. T., Biogenic synthesis of Au nanoparticles using vascular plants, *Industrial & Engineering Ehemistry Research*, *49* (24) (2010) 12762-12772.

[26] Firooz A. A., Mirzaie R. A., Kamrani F., Effect of morphological ZnO nanostructures on the optical and decolorization properties, *Journal of Structural Chemistry*, *59* (3) (2018) 739-743.

[27] Taghavi Fardood, S., Ramazani A., Asiabi P. A., Joo S. W., A novel green synthesis of copper oxide nanoparticles using a henna extract powder, *Journal of Structural Chemistry*, *59* (7) (2018) 1737-1743.

[28] Anbuvannan M., Ramesh M., Viruthagiri G., Shanmugam N., Kannadasan N., Anisochilus carnosus leaf extract mediated synthesis of zinc oxide nanoparticles for antibacterial and photocatalytic activities, *Materials Science in Semiconductor Processing*, *39* (2015) 621-628.

[29] Yuvakkumar R., Suresh J., Nathanael A. J., Sundrarajan M., Hong S. I., Novel green synthetic strategy to prepare ZnO nanocrystals using rambutan (*Nephelium lappaceum* L.) peel extract and its antibacterial applications, *Materials Science and Engineering: C*, *41* (2014) 17-27.

[30] Velmurugan P., Anbalagan K., Manosathyadevan M., Lee K. J., Cho M., Lee S. M., Oh B. T., Green synthesis of silver and gold nanoparticles using Zingiber officinale root extract and antibacterial activity of silver nanoparticles against food pathogens, *Bioprocess and Biosystems Engineering*, *37* (10) (2014) 1935-1943.

[31] Salam H. A., Sivaraj R., Venckatesh R., Green synthesis and characterization of zinc oxide nanoparticles from Ocimum basilicum L. var. purpurascens Benth.-Lamiaceae leaf extract, *Materials Letters*, *131* (2014) 16-18.

[32] Anžlovar A., Crnjak Orel Z., Kogej K., Polyol-mediated synthesis of zinc oxide nanorods and nanocomposites with poly (methyl methacrylate), *Journal of Nanomaterials*, *2012 (31)* (2012).

[33] Sharma V., Shukla R. K., Saxena N., Parmar D., Das M., Dhawan A., DNA damaging potential of zinc oxide nanoparticles in human epidermal cells, *Toxicology Letters*, *185* (3) (2009) 211-218.

[34] Nidhin M., Indumathy R., Sreeram K. J., Nair B. U., Synthesis of iron oxide nanoparticles of narrow size distribution on polysaccharide templates, *Bulletin of Materials Science*, *31* (1) (2008) 93-96.

[35] Anandalakshmi K., Venugobal J., Ramasamy V., Characterization of silver nanoparticles by green synthesis method using *Pedalium murex* leaf extract and their antibacterial activity, *Applied Nanoscience*, *6* (3) (2016) 399-408.

[36] Jayapriya M., Dhanasekaran D., Arulmozhi M., Nandhakumar E., Senthilkumar N., Sureshkumar K., Green synthesis of silver nanoparticles using *Piper longum* catkin extract irradiated by sunlight: antibacterial and catalytic activity, *Research on Chemical Intermediates*, *45*(6) (2019) 3617-3631.

[37] Kumar P., Suresh D., Nagabhushana H., Sharma S. C., *Beta vulgaris* aided green synthesis of ZnO nanoparticles and their luminescence, photocatalytic and antioxidant properties, *The European Physical Journal Plus*, *130* (6) (2015) 1-7.

[38] Jayappa M. D., Ramaiah C. K., Kumar M. A. P., Suresh D., Prabhu A., Devasya R. P., Sheikh S., Green synthesis of zinc oxide nanoparticles from the leaf, stem and in vitro grown callus of *Mussaenda frondosa* L.: characterization and their applications, *Applied Nanoscience*, *10* (8) (2020) 3057-3074.

[39] Azizi S., Mohamad R., Mahdavi Shahri M., Green microwave-assisted combustion synthesis of zinc oxide nanoparticles with *Citrullus colocynthis* (L.) Schrad: characterization and biomedical applications, *Molecules*, *22* (2) (2017) 301.

[40] Ananthalakshmi R., Rajarathinam S. R., Sadiq A. M., Antioxidant activity of ZnO Nanoparticles synthesized using peel extract, *Research Journal of Pharmacy and Technology*, *12* (4) (2019) 1569-1572.

[41] Safawo T., Sandeep B. V., Pola S., Tadesse A., Synthesis and characterization of zinc oxide nanoparticles using tuber extract of anchote (*Coccinia abyssinica* (Lam.) Cong.) for antimicrobial and antioxidant activity assessment. *Open Nano*, *3*, (2018) 56-63.